International Journal of Fatigue 76 (2015) 53–59

Contents lists available at ScienceDirect

International Journal of Fatigue

journal homepage: www.elsevier.com/locate/ijfatigue

Effect of sudden load decrease on the fatigue crack growth in cold drawn prestressing steel

J. Toribio [a,*], B. González [a], J.C. Matos [b], F.J. Ayaso [a]

[a] Department of Materials Engineering, University of Salamanca, E.P.S., Campus Viriato, Avda. Requejo 33, 49022 Zamora, Spain
[b] Department of Computing Engineering, University of Salamanca, E.P.S., Campus Viriato, Avda. Requejo 33, 49022 Zamora, Spain

ARTICLE INFO

Article history:
Received 30 October 2013
Received in revised form 5 December 2014
Accepted 6 January 2015
Available online 21 January 2015

Keywords:
Overload retardation effect
Loading sequences
Fatigue crack growth
Cold drawn prestressing steel
Crack tip opening displacement

ABSTRACT

This paper analyzes the overload retardation effect (ORE) on the fatigue crack growth (FCG) of cold drawn prestressing steel when different loading sequences are used. The ORE is more intense for elevated load decrease or for low initial stress intensity factor (SIF) range ΔK_0. A transient stage can be observed in the Paris curve (da/dN–ΔK) when the $K_{max}\Delta K$ value suddenly decreases, associated with the ORE and with the evolution of the plastic zone and compressive residual stresses near the crack tip. In tests with K_{max} decrease, a small zone appears related to FCG initiation, with a fatigue fractography resembling the tearing topography surface (TTS) mode, and associated with a decrease of crack tip opening displacement (CTOD).

1. Introduction

Fatigue crack growth (FCG) usually is generated by load sequences of random nature, thereby producing very complicated load spectra and often overload and underload phenomena. Therefore, variable amplitude loading sequences, depending of the combination of load parameters, specimen geometry, material properties, microstructure and environment, can produce retardation or acceleration with regard to FCG [1]. The cyclic plastic behaviour of the material is found to strongly affect the crack behaviour after an overload or an underload, the type of hardening is also of key importance: isotropic hardening is found to lower the effective part of the fatigue cycle, while kinematic hardening is found to increase it [2].

The appearance of an overload during fatigue produces retardation phenomena in the FCG. Such a deceleration reaches its maximum value after certain crack extension, asymptotically diminishing later up to a stabilized level [3], those phenomena being closely related to the residual plastic zone size [4]. The retardation effect is higher if the ratio of the maximum peak stress to the maximum baseline stress is increased [4] and if the baseline stress intensity factor (SIF) range ΔK is modified, either by increasing it (approaching the fracture toughness) or diminishing it (approaching the FCG threshold) [5].

Overload retardation effect (ORE) increases with the number of overload cycles [4,5] until it reaches a maximum value, existing a characteristic distance between overloads which ensures the greatest retardation effect [6]. In high-low block loading sequences the maximum ORE is instantaneous [5]. A single compressive peak load just after the tensile overload relaxed the overload effect [3] and can result in an acceleration in the rate of FCG [7].

The main reason for the retardation in overload crack advance, as well as the crack tip closure, are the crack branches and the contact between surfaces, of rough fracture, after overload [8]. The ORE is higher due to plasticity effects (for elevated ΔK) or because of asperity wedging (for low ΔK) [5]. A block of compressive overload cycles may cause ORE on the growth rate of the initial crack, due to the oxide-induced closure which generates debris [9]. On the other hand, other authors maintain that every deviation of large crack growth behaviour can be linked to the presence of residual stresses on the material [10].

This paper considers the two main driving forces for FCG: (i) the SIF range ΔK and (ii) the maximum SIF K_{max} [11], and analyzes the ORE caused by the sudden decrease of any of them on the FCG in cold drawn pearlitic steels. To this end, the following factors were considered: the ORE during FCG, the plastic zone size in the close vicinity of the crack tip, the appearance of the micro-tearing pattern in the fatigue fracture surface and the crack tip opening displacement (CTOD).

---

[*] Corresponding author. Tel.: +34 (980) 54 50 00; fax: +34 (980) 54 50 02.
E-mail address: toribio@usal.es (J. Toribio).

http://dx.doi.org/10.1016/j.ijfatigue.2015.01.007
0142-1123/© 2015 Elsevier Ltd. All rights reserved.

2. Experimental procedure

The material used in the study was high strength prestressing steel with eutectoid composition (0.789 wt.% C, 0.681 wt.% Mn, 0.210 wt.% Si, 0.218 wt.% Cr, 0.061 wt.% V, balanced with Fe) and pearlitic microstructure. Commercial prestressing steel wires are obtained from a hot rolled bar which is subjected to a cold drawing process in seven steps, thereby producing a high cumulative plastic strain ($\varepsilon^P = 1.6$) and activating a strain hardening mechanism to improve the conventional mechanical properties of the material. The resulting mechanical properties are as follows: yield strength $\sigma_Y = 1480$ MPa, tensile stress $\sigma_R = 1820$ MPa and Young modulus $E = 209$ GPa.

Fatigue tests were performed on wires of 300 mm of length and 5.1 mm of diameter, subjected to two cyclic loading sequences, each of one consisting of maintaining constant the two key mechanical parameters defining the fatigue cycle, namely (i) the stress range $\Delta\sigma$ and (ii) the maximum stress $\sigma_{\max}$ (and obviously $\sigma_{\min}$), and a sudden decrease of either $\Delta\sigma$ or $\sigma_{\max}$ in the transition from the first to the second stage of loading. An axial cyclic tensile load was externally applied under a frequency of 10 Hz and using a sinusoidal wave in such a manner that the maximum stress was always maintain well below the material yield strength σ_Y. An extensometer of 25 mm gage length was placed on the specimen in symmetrical position in relation to the crack mouth, in order to monitor the crack length by means of the compliance ($C = u/F$, ratio of the relative displacement measure by the extensometer and the externally-applied remote tensile load). The designed test types appear sketched in Fig. 1: (i) in type A tests there is a decrease of maximum stress $\sigma_{\max}$; (ii) in type B tests there is a decrease of stress range $\Delta\sigma$; (iii) in type C tests there is a decrease of both driving forces ($\sigma_{\max}$ and $\Delta\sigma$). In all types of tests (A, B and C) the subindex indicates the percentage of decrease in relation to the previous value.

The fracture surface corresponding to the sudden load changes was observed by optical microscopy and by scanning electron microscopy (SEM). Materialographic techniques (mounting, grinding, polishing and 5% Nital etching) were used to observe by SEM the microstructure of the prestressing steel. In addition, a fracto-materialographic procedure was used to evaluate the fatigue crack paths by interrupting the test before final fracture, cutting the specimen across a plane perpendicular to the crack front and applying metallographic techniques to observe the evolution of the crack immersed in the microstructure.

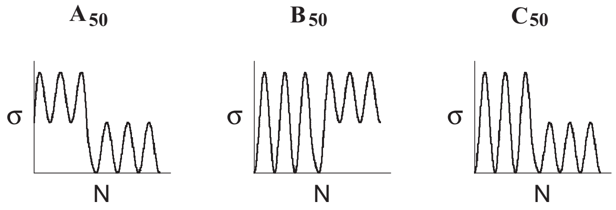

Fig. 1. Tests with 50% sudden load decrease.

3. Experimental results

3.1. Microstructural analysis

The microstructure of prestressing steel is constituted by pearlite colonies, each of one consisting of alternate lamellae of ferrite and cementite with common orientation inside the colony (such an orientation being different from that of the lamellae contained in any neighbourhood colony). Cold drawing produces effects in the two basic microstructural levels of the steels, namely, the pearlitic colony and the ferrite/cementite lamellae.

With regard to the first microstructural level (the pearlitic colony), there is a progressive orientation [12] with cold drawing (in direction quasi-parallel to the wire axis or drawing direction), together with a slenderization in the same direction [13]. While in the first stages of drawing the orientation effect is predominant, in the last drawing steps a marked slenderization and enlargement of the colonies takes place [12,13].

In the matter of the second microstructural level (the set of pearlitic lamellae), again a progressive orientation [14] appears with cold drawing (in direction quasi-parallel to the wire axis or drawing direction), in addition to the increase of packing closeness in the form of reduction of the interlamellar spacing of pearlite [15]. Whereas in the earlier steps of the process the orientation effect is relevant, in the further stages of drawing a marked decrease of spacing appears (accompanied by curling of the lamellae), cf. [14,15].

Fig. 2 shows the microstructure of prestressing steel wire in both transversal and longitudinal sections, where the afore-said effects associated with the final step of drawing (heavily drawn prestressing steel wire) can be observed, namely orientation of colonies and lamellae, reduced interlamellar spacing and enlargement of the colonies in the drawing direction.

3.2. Retardation in fatigue crack growth (FCG)

The FCG curve in the Paris regime, cyclic crack growth rate (CCGR) *vs.* the SIF range da/dN–ΔK, for the cold drawn pearlitic steel analyzed in this paper is shown in Fig. 3. The plot is the same for different values of the R ratio [16]; so CCGR depends mainly on the SIF range, while the maximum SIF during fatigue, $K_{\max}$, is almost irrelevant. The Paris fitting gives coefficients C and m of

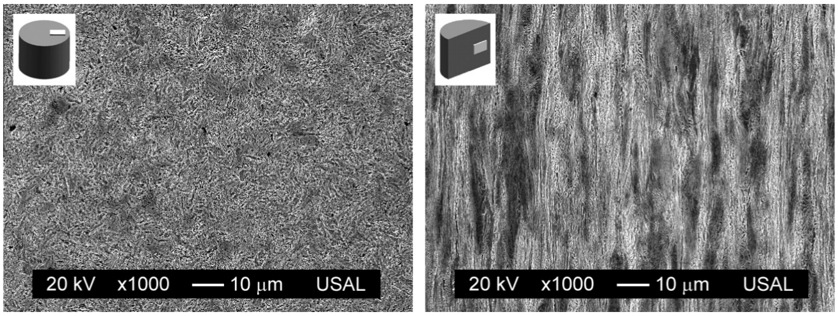

Fig. 2. Microstructure of prestressing steel wire: in the transversal section (left) and the longitudinal section (right). The horizontal side of the photograph is associated with the radial direction in the wire, whereas the vertical side of the photograph corresponds to the circumferential direction in the transversal section and to the axial direction in the longitudinal section.